



ELSEVIER

Journal of Chromatography A, 708 (1995) 41–53

JOURNAL OF  
CHROMATOGRAPHY A

# Study of radial compression high-performance liquid chromatographic columns for preparative chromatography

David P. Gervais<sup>1</sup>, W. Scott Laughinghouse, Giorgio Carta\*

*Center for Bioprocess Development, Department of Chemical Engineering, University of Virginia, Charlottesville, VA 22903-2442, USA*

First received 31 January 1995; revised manuscript received 14 March 1995; accepted 14 March 1995

## Abstract

The operating characteristics and efficiency of a preparative-scale, radial compression chromatograph are studied. Two commercial  $C_{18}$  silica packings are used, one irregular and one spherical and monodispersed. For each packing, the relationship between mobile phase flow-rate, column backpressure, and radial compression pressure is determined. A model is proposed to explain this relationship and determine the radial compression pressure needed to maintain the column effectively compressed at each operating flow-rate. The chromatographic efficiency of these columns is also determined. When an adequate radial compression level is used, the efficiency of the preparative-scale system is nearly the same as that of analytical-scale columns. Applying incremental levels of radial compression can also lead to a restoration of the efficiency of columns whose performance was degraded by operation at low radial compression pressures.

## 1. Introduction

Both in analytical and preparative chromatography it is desirable to utilize packed columns which are radially homogeneous and structurally stable in order to insure a uniform and constant flow of mobile phase throughout the column's cross section. Advances in media morphology and packing techniques have made it possible to obtain highly efficient small diameter columns, suitable for analytical applications. However, obtaining uniform and stable packings for HPLC in preparative-scale equipment, 5 cm in diameter or larger, frequently requires the use of special

hardware. Several authors [1–5] have reviewed hardware and operating techniques designed to operate reliably large-scale HPLC columns, which generally rely on the application of axial or radial compressive forces to the packed bed. However, it appears that even utilizing such compression techniques, completely homogeneous bed structures are not necessarily obtained. Marme et al. [6], for example, studied 5-cm diameter axial compression columns by NMR imaging and found their columns to be inhomogeneous, with some regions containing 10–20% more mobile phase than others. They also obtained SEM images of cross-sections of extruded columns and determined that they contained denser areas of packing near the core than at the wall regions of the bed.

The static and dynamic behavior of packed

\* Corresponding author.

<sup>1</sup> Current address: Pfizer Inc., Groton, CT, USA.

beds under compressive stresses are extremely complex and little information is available in the chromatography literature. Evidence of such complexity may be found, however, in the powder-compaction literature. For example, Train [7] discusses the pressure and density gradients formed in a mass of packed powder undergoing mechanical compaction from the application of a uniaxial pressure. Train obtained pressure profiles within cylindrical powder compacts obtained by compression with a moving piston and die assembly utilizing manganin wire resistance gauges at different radial and axial positions. He also obtained density profiles by sectioning the powder compacts and measuring the mass of powder in each layer. Train's results show extremely complicated pressure and density profiles for uniaxially applied pressures in the range 2.79–200 MPa. At low compression loads, larger pressure and packing densities were found in regions near the piston surfaces closest to the die walls, with the concurrent formation of a lower pressure, lower density core near the center. Both pressure and density decreased from the piston surface to the die bottom. For higher compression loads, even more complicated patterns were seen, with the development of higher pressure, higher density regions in the center of the compact, surrounded by lower density regions.

To our knowledge, similar detailed studies of pressure and density profiles for compressed chromatography columns are currently not available. However, a number of studies are available addressing the operating characteristics and chromatographic performance of such columns. For example, radial compression columns, which are considered in this paper, have been the subject of two recent investigations. Carta and Stringfield [8] have studied a radial compression preparative chromatography system utilizing columns 10 cm in diameter and 60 cm in length. This study, focussed on packings 30  $\mu\text{m}$  in size or larger, found that efficiencies close to those attained in analytical columns could be obtained by applying an appropriate amount of radial compression. Furthermore, it was found that through the application of incremental levels of

radial compression, the efficiency of a column whose performance had deteriorated could be almost completely restored. It was also noted, that when these columns are operated at different flow-rates with a constant amount of bed compression, the net compressive force on the bed decreases as the flow-rate of the mobile phase is increased. Thus, in general it is necessary to increase the radial precompression pressure when the column is operated at higher flow-rates. Similar conclusions were reached by Sarker and Guiochon [9] who studied a 7.5-cm diameter, 17.5 cm long radial compression chromatography system with cartridges packed with a 16.5- $\mu\text{m}$  diameter  $\text{C}_{18}$  silica packing. On the basis of chromatographic experiments they concluded that these packings exhibit little radial heterogeneity and that channels formed in columns whose performance had deteriorated could be repaired by applying elevated radial compression pressures.

In this study we have extended our previous investigation with 10-cm diameter columns to a radial compression unit similar to the one used by Sarker and Guiochon. We have considered reversed-phase chromatography packings with different particle sizes, one comprising irregular silica particles and the other comprising spherical silica. For each packing we have determined the relationship between flow-rate, column pressure, and radial compression pressure, and the chromatographic efficiency for a model separation.

## 2. Experimental

### 2.1. Equipment and methods

The experimental apparatus consisted of a Biotage KPCM 100 radial compression module and a Biotage Kiloprep 100 (KP 100G Prep LC) pumping station (Biotage, Charlottesville, VA, USA) and is similar to the apparatus described by Sarker and Guiochon [9]. The KPCM 100 compression module accepts 7.5 cm I.D., 9.5 cm O.D. radial compression cartridges with nominal lengths up to 30 cm. In this work we used medium-density food-grade polyethylene car-

tridges packed to a length of 17.5 cm (Biotage). Each cartridge is fitted with identical flow distributors at each end and with a set of two porous polyethylene frits, 40 and 10  $\mu\text{m}$ , for flow distribution and containment of the packing. One cartridge was packed with Waters Bondapak,  $C_{18}$ , 15–20  $\mu\text{m}$ , 125 Å nominal pore size, irregular silica (Waters, Milford, MA, USA). This cartridge had a manufacturer-recommended radial compression of 200 psig (1.38 MPa). The second cartridge was packed with Shandon Hyperprep,  $C_{18}$  silica (Shandon Scientific, Cheshire, UK). This packing is spherical and mono-dispersed, with a nominal 12- $\mu\text{m}$  particle size. The manufacturer-recommended radial compression pressure was 225 psig (1.55 MPa). The equipment was set up by inserting the cartridge in the radial compression system and sealing the chamber. Before establishing flow of the mobile phase, the cartridge was then pressurized by introducing radial compression fluid in the annular space between the cartridge outer wall and the chamber wall until a desired precompression pressure was achieved. The radial compression fluid was then isolated with the valve system. Thus, the compression module was operated essentially as a constant-volume system.

The column inlet pressure and the pressure in the radial compression chamber were monitored with a bank of three pressure gauges with ranges 0–300, 0–600, and 0–3000 psig. Actual pump flow-rates were measured at each nominal setting by collecting the column effluent in a graduated cylinder for fixed periods of time.

Some experiments were also done with analytical-scale columns (0.46 cm I.D., 25 long stainless steel columns) (Biotage), packed with the same packing materials contained in the preparative cartridges. The apparatus described in Ref. [8] was used for these experiments.

## 2.2. Chromatographic experiments

Isocratic elution experiments were carried out by injecting 1-ml samples of a mixture containing 1.2 g/l each of *p*-hydroxybenzoic acid methyl ester (methyl paraben) and ethyl ester (ethyl paraben) in a 50:50 (v/v) methanol–water mo-

bile phase. Methyl and ethyl paraben were obtained from Sigma Chemical Co. (St. Louis, MO, USA) and HPLC-grade methanol was obtained from Baxter Scientific (Muskego, MI, USA).

Elution profiles were determined by passing the column effluent through a Waters Model 481 chromatographic detector (Waters, Milford, MA, USA) fitted with a preparative flow cell. The detector millivolt signals at a wavelength of 254 nm were collected with a microcomputer-based data acquisition system and stored for subsequent calculations.

The chromatographic efficiency of these columns was evaluated by calculating the first and second statistical moments of the digitized response peaks of methyl and ethyl paraben. The two coinjected solutes were always completely separated in these experiments. Thus, their individual peak properties could be determined accurately. For each flow-rate studied, extracolumn retention and dispersion effects were also evaluated by making identical injections without the column. In this case, the inlet and outlet lines were connected together with a Swagelock connector. The first moment and variance of peaks obtained in this configuration were subtracted from those of peaks obtained with the column on-line to obtain the true retention time and height equivalent of theoretical plates (HETP) for each component as described by Carta and Stringfield [8]. It should be noted that since the moment method was used, the resulting HETP values are higher than those that would be obtained by other methods based on average peak properties even if the peaks obtained in this work were generally relatively symmetrical. Asymmetry factors were obtained graphically at 10% of peak height.

## 3. Results and discussion

### 3.1. Pressure relationships

Figs. 1a and 2a show the column backpressure (corrected for extracolumn effects) as a function of the mobile phase flow-rate for the Bondapak

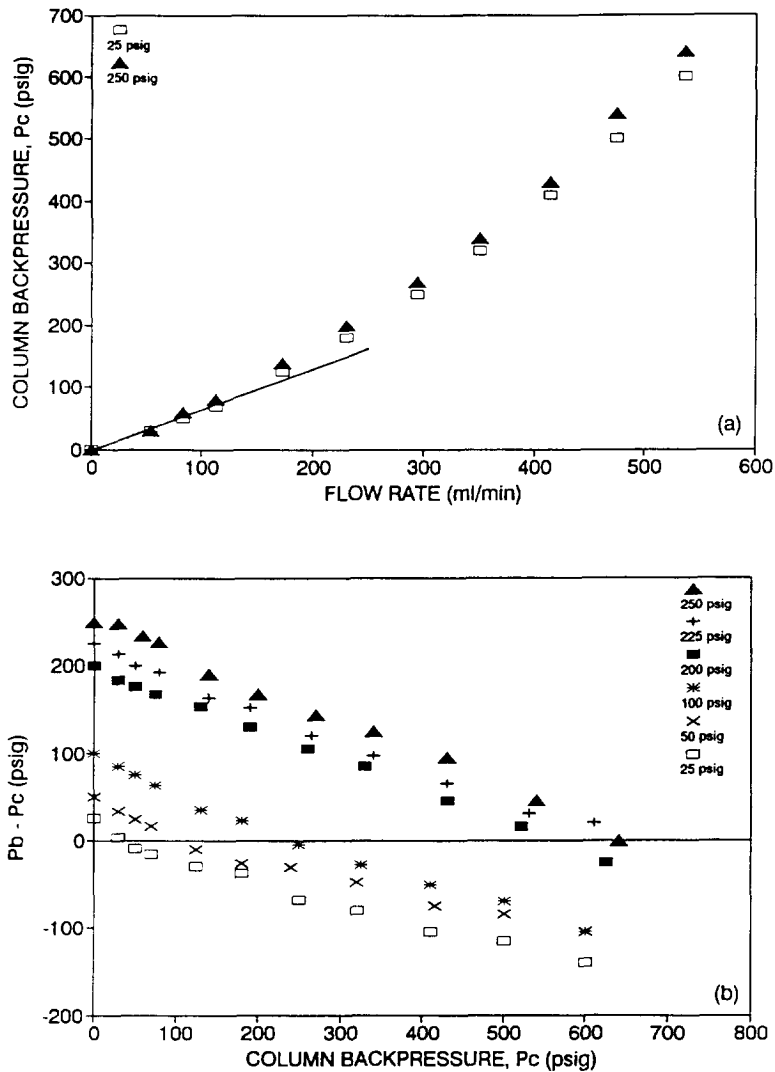


Fig. 1. Column backpressure (a) and difference between the radial compression pressure and the column pressure (b) for different precompression settings. Data for Bondapak cartridge with a methanol–water (50:50, v/v) mobile phase. Pressure values are given in relative gauge pressure readings (1 psig  $\sim$  0.0069 MPa).

and the Hyperprep cartridges at the highest and lowest values of precompression pressures used for each. In each case, although not shown for clarity, intermediate precompression pressures yielded experimental points intermediate between those shown in the figures. The curves are not straight for either packing in spite of the fact that the flow is laminar. Sarker and Guiochon [9]

have obtained an approximate linear relationship for a similar system. However, the data reported by these authors were limited to a maximum flow-rate of ca. 275 ml/min. From Figs. 1 and 2, it is apparent that a large deviation from linearity is not seen until higher flow-rates are reached. The curvature is somewhat greater for the irregular packing (Fig. 1a) than for the spherical

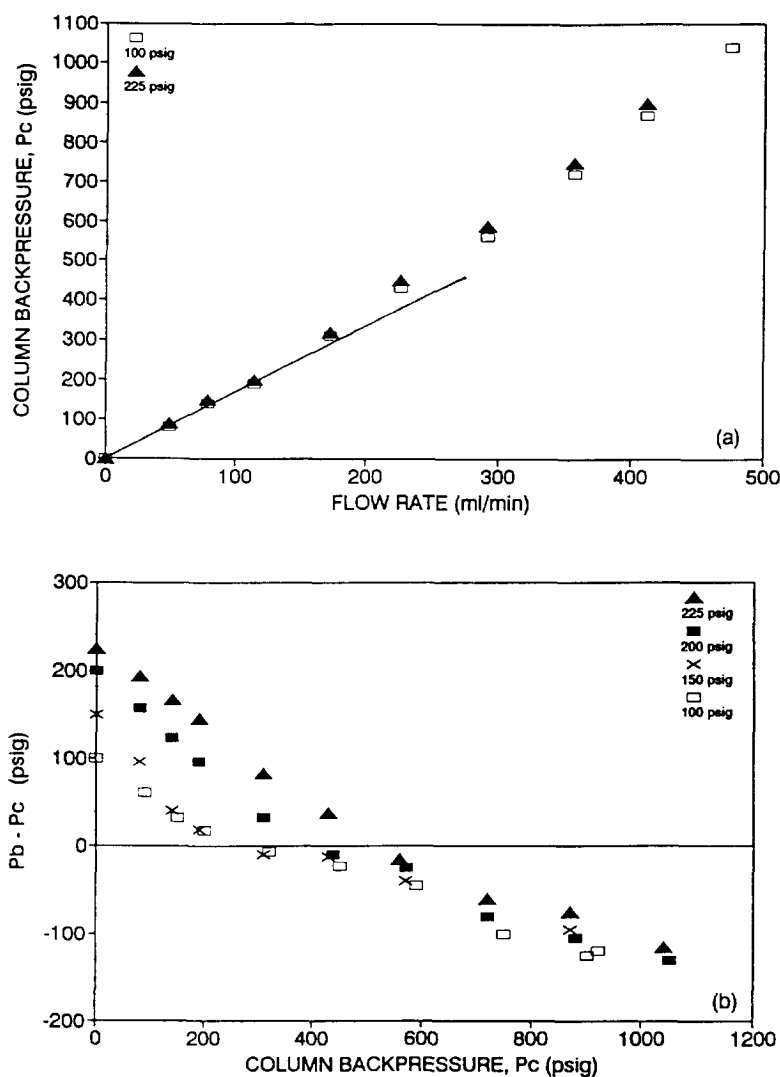


Fig. 2. Column backpressure (a) and difference between the radial compression pressure and the column pressure (b) for different precompression settings. Data for Hyperprep cartridge with a methanol–water (50:50, v/v) mobile phase. Pressure values are given in relative gauge pressure readings (1 psig  $\sim$  0.0069 MPa).

material (Fig. 2a). A linear regression of the initial slope of these curves with the Blake–Kozeny equation [10]

$$\frac{P_c}{L} = \frac{150(1-\epsilon)^2}{\epsilon^3 d_p^2} \mu u \quad (1)$$

where  $\epsilon$  is the column void fraction,  $d_p$  the

particle diameter,  $\mu$  the mobile phase viscosity, and  $u$  the superficial velocity, is also shown in these figures. This fit yielded values of  $\epsilon = 0.370$  for the Bondapak cartridge and  $\epsilon = 0.344$  for the Hyperprep cartridge using particle diameters of 17.5 and 12  $\mu\text{m}$  respectively.

The difference between the pressure in the radial compression fluid,  $P_b$ , and the column

backpressure,  $P_c$ , obtained for each precompression level is shown in Figs. 1b and 2b. Since the pressure of the radial compression fluid is uniform along the length of the cartridge while the mobile phase pressure decreases from entrance to exit, this differential pressure corresponds to the minimum net radial compressive stress applied to the cartridge. Since these experiments are carried out with a constant volume of radial compression fluid in the chamber,  $P_b$  increases with mobile phase flow-rate as the cartridge becomes gradually expanded near the column entrance. Thus, for each flow-rate (and corresponding backpressure value) there is a greater net compressive stress near the column exit than near the entrance. When the precompression level is low, the differential pressure  $P_b - P_c$  becomes negative at high flow-rates. For these conditions the cartridge is expanded near the entrance relative to its initial precompressed state. The existence of such a non-uniform compressive stress, previously noted by Carta and Stringfield, may indicate that these radially compressed cartridges are not completely homogeneous in the axial flow direction. This may also explain qualitatively the origin of the pressure-flow relationship seen experimentally. It is well known that the void fraction has a very large non-linear effect on the pressure drop in packed beds, *i.e.* the pressure drop increases rapidly as the void fraction is reduced to small values. In the radial compression cartridges, as the mobile phase flow-rate is increased for a given precompression pressure, an increasing portion of the packing near the exit attains higher levels of radial compression relative to regions near the entrance, since near the exit the radial pressure differential is maximum. This exit portion of the packing is thus denser and is likely to have a considerably lower hydraulic permeability than regions near the entrance. Thus, the existence of a highly compacted region may explain the curvature in the pressure-flow-rate relationship noted when the column is operated with a constant precompression pressure.

Carta and Stringfield have previously noted that in a 10-cm diameter radial compression column there existed a simple asymptotic rela-

tionship between the difference  $P_b - P_c$  and the column backpressure  $P_c$

$$P_b - P_c = P_b^0 - \frac{1}{2} P_c \quad (2)$$

where  $P_b^0$  is the radial precompression pressure. This asymptotic relationship was derived theoretically by assuming that the pressure within the packing varies linearly over its length and that the packed cartridge behaves like an elastic body with a constant compressibility. Although on a detailed level the mechanical behavior of the packed cartridges is likely very different from the assumptions made, the trends predicted by this equation are quite consistent with the experimental data shown in Fig. 2a,b. The trend, however, changes with  $P_b - P_c$  becomes negative and the slope of the curves becomes much smaller. For these conditions, a portion of the cartridge near the entrance is expanded. Since the total column value and the volume of the radial compression fluid are essentially constant after the initial precompression, it is apparent that there must be a radial expansion of the cartridge near the column entrance and a contraction near the column exit. If the column pressure varies linearly within the column, at a distance

$$z' = \frac{L(P_c - P_b)}{P_c} \quad (3)$$

the net compressive stress on the cartridge is zero and so is its deformation. Using elementary stress-strain relationships, the change in radius of the cartridge relative to the radius of the uncompressed cartridge and before a flow of the mobile phase is established is given by

$$\Delta R^0 = \frac{R}{E} P_b^0 \quad (4)$$

where  $E$  is a bulk modulus of elasticity of the packed cartridge and  $R$  is the cartridge radius. When flow is established, a pressure  $P_i(z)$  exists at each point within the column. For these conditions the radial deformation of the cartridge can be approximated by

$$\Delta R'(z) = \frac{R}{E'} [P_b - P_i(z)] \text{ for } 0 < z < z' \quad (5)$$

$$\Delta R(z) = \frac{R}{E} [P_b - P_i(z)] \text{ for } z' < z < L \quad (6)$$

$E'$  is likely to be considerably smaller than  $E$ . In fact, since the packed bed has obviously little or no tension strength, when  $P_b - P_i$  is negative only the cartridge shell is resisting expansion. In order to maintain the total volume constant, the following relationship must be satisfied

$$\int_0^{z'} \Delta R'(z) dz + \int_{z'}^L \Delta R(z) dz = L \Delta R'' \quad (7)$$

Substituting Eqs. 4, 5 and 6 in Eq. 7 and integrating, we obtain the result

$$P_b - P_c = \left\{ \left[ \frac{E}{E'} P_c^2 + 2 \left( 1 - \frac{E}{E'} \right) P_b^0 P_c \right]^{1/2} - P_c \right\} / \left( 1 - \frac{E}{E'} \right) \quad (8)$$

which is valid when  $0 < z' < L$ . A plot illustrating the behavior predicted by this equation is shown in Fig. 3a for an assumed initial precompression pressure of 100 psig and different values of the  $E/E'$  ratio. All the curves merge asymptotically to the trend predicted by Eq. 3 when the backpressure is such that  $P_b - P_c = 0$ . For lower backpressures the cartridge is compressed along its entire length. The fraction of the cartridge under positive compression,  $z'/L$ , is also shown in Fig. 3b for the same conditions. We see that when  $E/E'$  is small (the cartridge shell is very stiff or the packing is highly compressible) a significant portion of the cartridge would be expanded, rather than compressed. This, of course, could be remedied by raising the radial compression pressure through the introduction of additional radial compression fluid.

It is obviously difficult to calculate  $E$  a priori. Thus, values of  $E/E'$  were determined by fitting Eq. 8 to the experimental data shown in Figs. 1b and 2b. A value of  $E/E' = 15$  provided a good fit of all the data for the Bondapak cartridge, while a value of  $E/E' = 30$  provided a good fit for the Hyperprep cartridge. A comparison of the experimental data obtained at each precompression level with the curves calculated from Eq. 8 for these values of  $E/E'$  is given in Figs. 4 and 5.

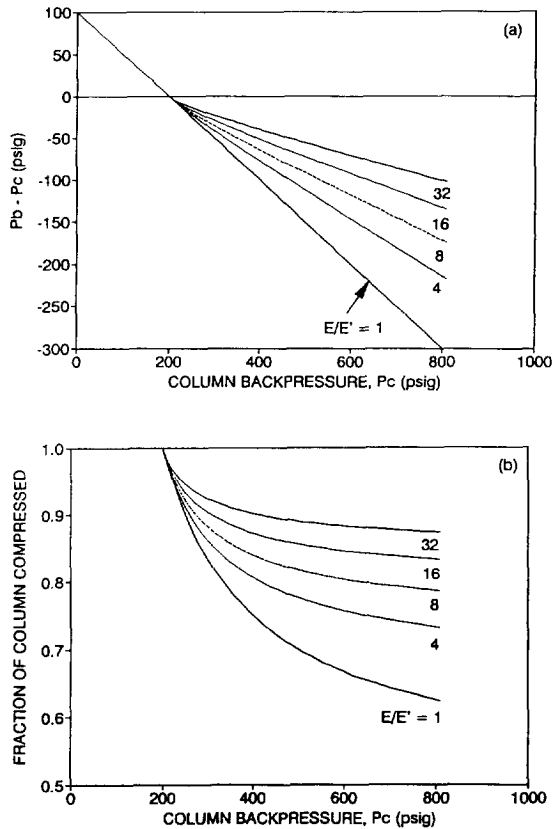


Fig. 3. Effect of column backpressure on minimum net radial compression (a) and fraction of column compressed (b) according to Eqs. 2 and 8 for different values of  $E/E'$ .

The fact that  $E/E'$  is larger for the smaller and uniformly sized Hyperprep media is perhaps consistent with the expected lower compressibility and denser initial packing of this material. Clearly, at the radial compression pressures considered, the compressibility of the silica particles is insignificant. Thus, the volume changes that occur when compressing the cartridges must result from elimination of interparticle voids. The mechanism through which this occurs is likely to be much more complicated than that suggested by the assumptions underlying Eqs. 2-8. These equations, however, do capture the main experimental traits, indicating that although perhaps not mechanistically correct, they permit a reasonable representation of the various factors by lumping all contributions in the single parameter  $E/E'$ .

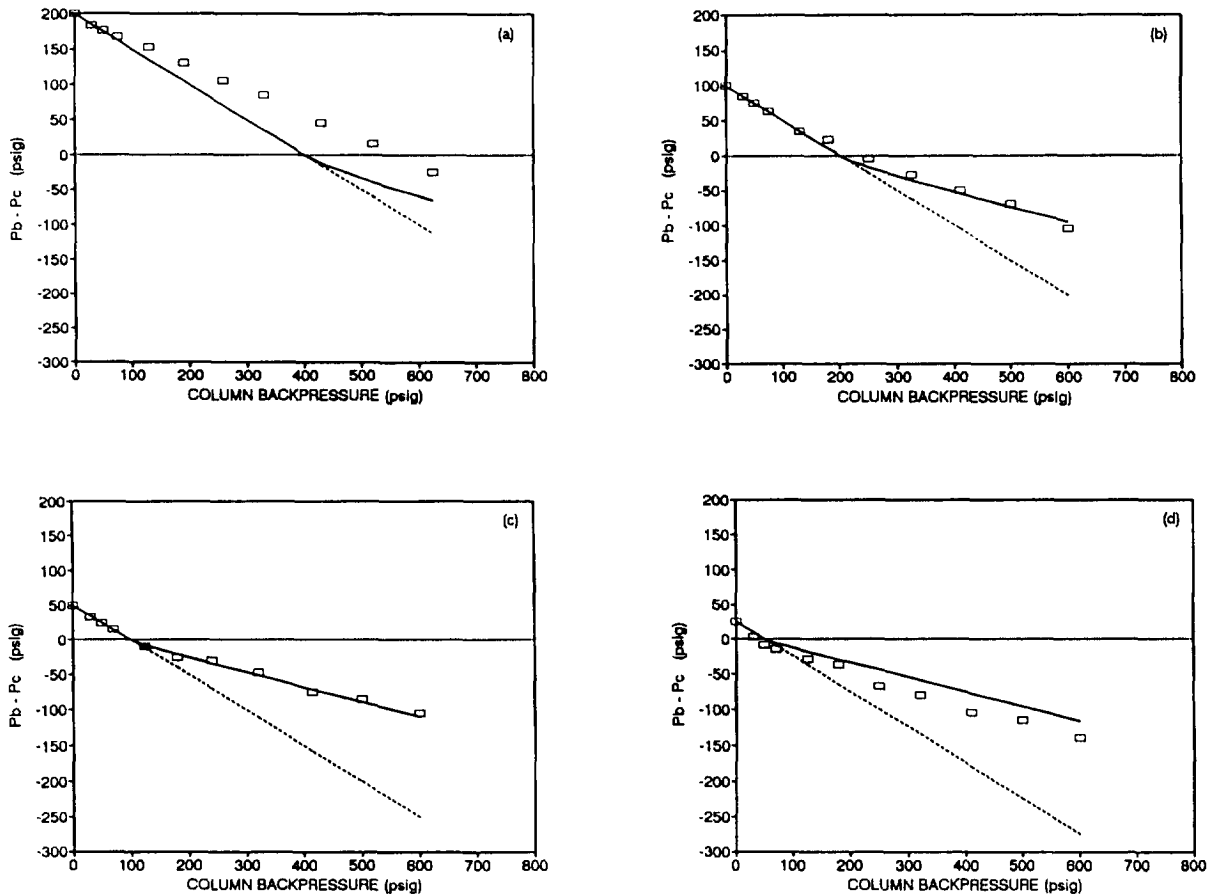


Fig. 4. Comparison of predictions of Eqs. 2 and 8 for  $E/E' = 15$  with experimental data for the Bondapak cartridge at different precompression pressures. (a) 200, (b) 100, (c) 50, (d) 25 psig.

### 3.2. Column efficiency

Chromatography experiments were conducted with methyl and ethyl paraben mixtures in a 50:50 (v/v) methanol–water mobile phase at room temperature ( $22 \pm 2^\circ\text{C}$ ) both in the analytical-scale columns and with the preparative-scale radial compression cartridges. In the analytical-scale column, the measured retention factors were 4.9 for methyl paraben and 8.5 for ethyl paraben with the Bondapak packing, based on an assumed void fraction of 0.4. Somewhat lower values of 3.3 and 5.9, respectively for methyl and ethyl paraben, were found for the Hyperprep packing. The ratio of retention factors for the two solutes is essentially the same

for both media, indicating that the two packings have similar selective adsorptive properties, but a somewhat different adsorption capacity. In both cases, a plot of the logarithm of the retention factor versus the logarithm of the methanol mole fraction was linear [11]. Similar retention factors were obtained with the preparative-scale cartridges.

The efficiency of each radial compression cartridge was assessed in a series of isocratic elution runs. For each set of runs, a radial precompression pressure was set in the absence of flow and injections were then performed at different flow-rates before setting the precompression pressure to a new level for the next set of runs.



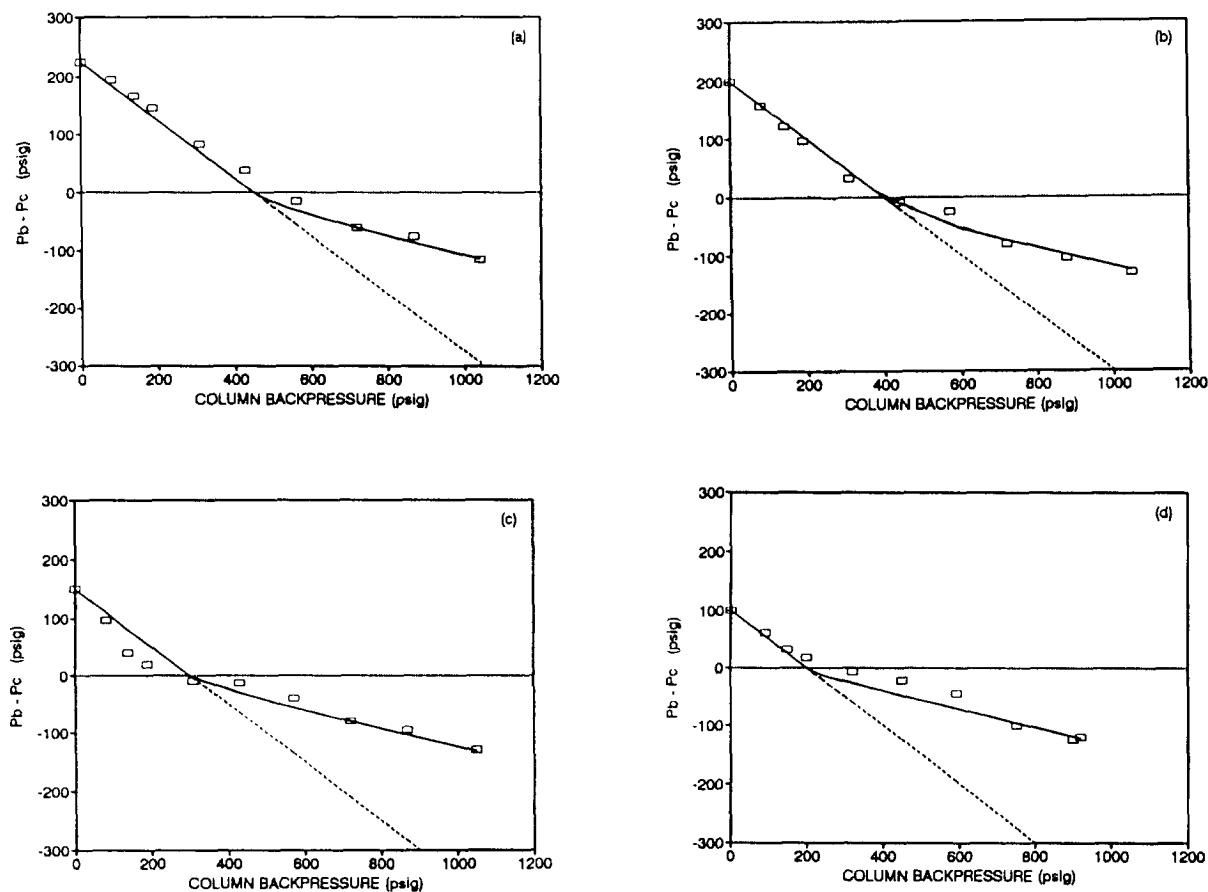


Fig. 5. Comparison of predictions of Eqs. 2 and 8 for  $E/E' = 30$  with experimental data for the Hyperprep cartridge at different precompression pressures. (a) 225, (b) 200, (c) 150, (d) 100 psig.

The reduced HETP ( $h = H/d_p$ , based on  $d_p = 17.5 \mu\text{m}$ ) obtained with the Bondapak cartridge is shown in Fig. 6a,b for methyl and ethyl paraben as a function of the reduced velocity,  $v' = vd_p/D$  for flow-rates in the range 43–500 ml/min. The reduced velocity was calculated using the mobile diffusivity values  $D = 4.6 \times 10^{-6}$  and  $D = 5.0 \cdot 10^{-6} \text{ cm}^2/\text{s}$  for methyl and ethyl paraben at  $22^\circ\text{C}$ , respectively. These values were estimated using the data of Huss et al. [12] for the diffusivity of benzaldehyde in water-methanol mixtures correcting for the difference in molar volume of this solute and the solutes used in our work on the basis of the Wilke-Chang equation. In these figures the data for the preparative radial compression cartridge are

shown in comparison with the corresponding data for the analytical-scale column. It appears that the column efficiency is essentially independent of precompression pressure for the preparative cartridge and virtually the same as the efficiency of the analytical column. Fairly sharp and symmetrical peaks were obtained for the conditions shown in this figure. The plate counts were  $N > 11\,700$  plates/m at 53 ml/min and  $N > 8000$  plates/m at 400 ml/min. Peak asymmetry factors were between 1.2 and 1.5 for all of the conditions shown in these figures.

The Knox parameters derived from a fit of the preparative-scale HETP values are  $a = 2.2$ ,  $b = 12$ , and  $c = 0.16$  for methyl paraben and  $a = 2.0$ ,  $b = 13$ , and  $c = 0.14$  for ethyl paraben. The  $a$ -

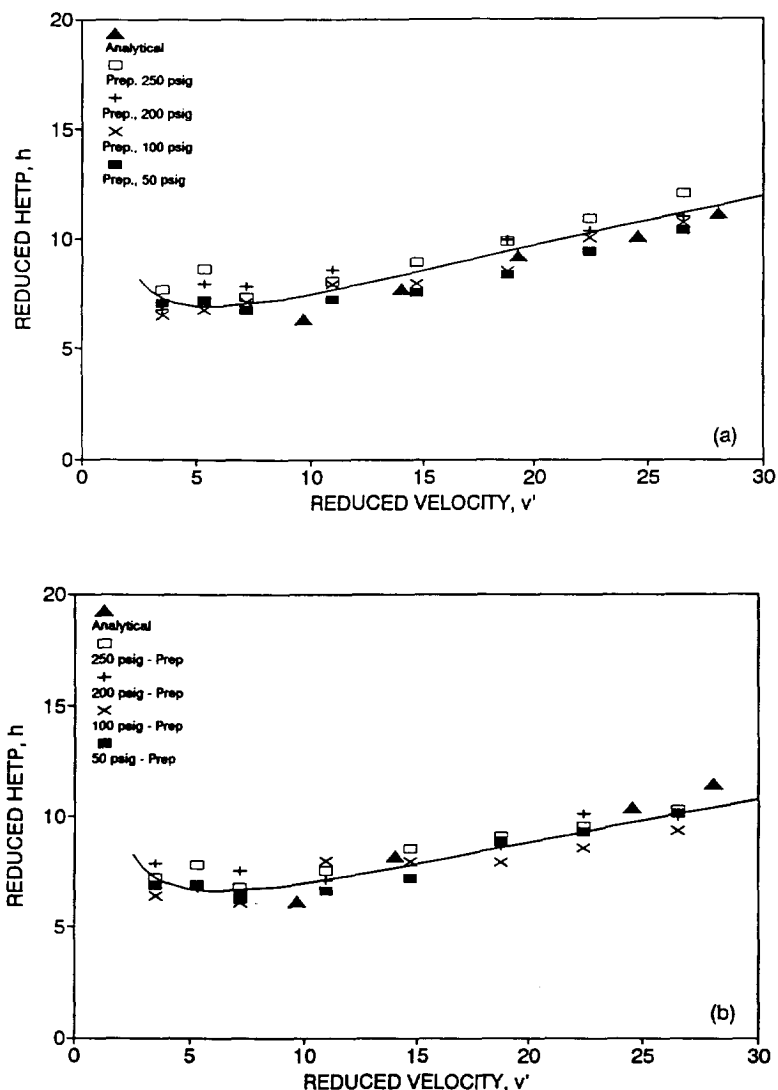


Fig. 6. Reduced HETP as a function of the reduced velocity for different precompression settings with the Bondapak preparative cartridge and for an analytical-scale column. (a) Methyl paraben, (b) ethyl paraben. All measurements for a methanol-water (50:50, v/v) mobile phase.

values are quite small and the  $c$ -values are in the range normally found for porous packings. However, the  $b$ -values are quite large. These results, obtained for reduced velocities in the range 3–30, are consistent with those of Sarker and Guiochon. For a  $16.5\text{-}\mu\text{m}$  reversed-phase silica packing with reduced velocities between 3 and 11, they found values of  $a$  between 0.6 and 8, values of  $b$  between 0.7 and 60, and values of  $c$

between 0.04 and 0.19. Obviously, the inordinately high  $b$ -value has little effect at high mobile phase velocities. Indeed, at reduced velocities greater than 10, the preparative-scale cartridges have an efficiency very close to those of analytical columns.

The precompression pressure value was found to have a far greater effect for the Hyperprep cartridge. This cartridge was initially operated at

the manufacturer-recommended precompression pressure of 225 psig. At this precompression level, the cartridge was essentially as efficient as an analytical-scale column packed with the same material as is shown in Fig. 7. The Knox parameters determined from a fit of the radial compression column data for both methyl and ethyl paraben were  $a = 0.19$ ,  $b = 16$ , and  $c = 0.35$ . Only at very low flow-rates are the reduced HETP values of the preparative-scale column greater than those of the analytical-scale one. Accordingly the Knox parameter  $b$  has a large value. Chromatograms obtained for this cartridge at the initial precompression setting are shown in Fig. 8, for a low and a high flow-rate. For these conditions very sharp and nearly symmetrical peaks are obtained, consistent with those obtained in the analytical column with this packing. When the precompression pressure was subsequently reduced to 100 psig, however, the cartridge efficiency was severely degraded. This is shown in Fig. 9 which portrays the elution profiles obtained for injections identical to those in Fig. 8, but for this reduced precompression

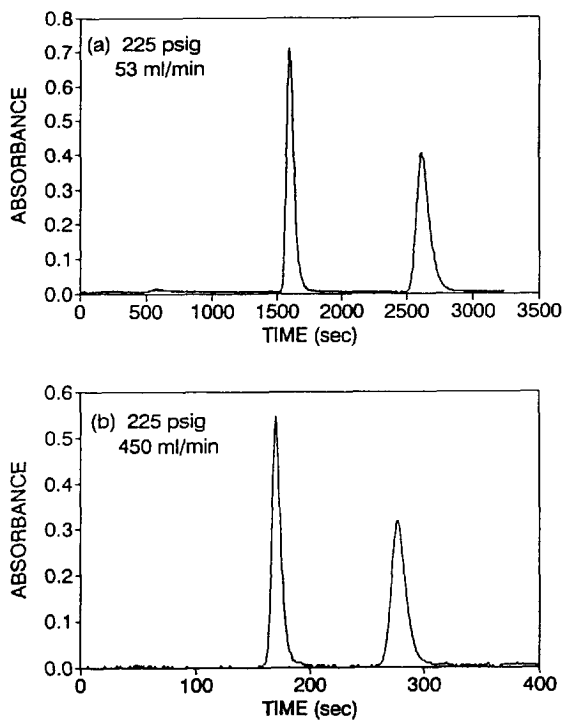


Fig. 8. Elution profiles for methyl and ethyl paraben with the Hyperprep cartridge at the initial precompression setting of 225 psig. (a)  $H = 0.0081$  cm and  $\alpha_s = 1.9$  for methyl paraben,  $H = 0.0085$  cm and  $\alpha_s = 1.8$  for ethyl paraben, (b)  $H = 0.0012$  cm and  $\alpha_s = 1.3$  for methyl paraben,  $H = 0.0099$  cm and  $\alpha_s = 1.7$  for ethyl paraben.

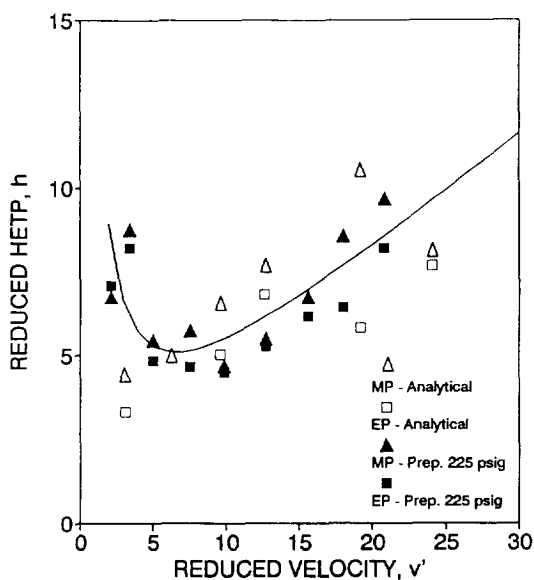


Fig. 7. Reduced HETP as a function of the reduced velocity with the Hyperprep preparative cartridge at a 225 psig precompression and for an analytical-scale column. Data for methyl paraben (MP) and ethyl paraben (EP). All measurements for a methanol–water (50:50, v/v) mobile phase.

level. At the lower flow-rate, the peaks are severely distorted, and they begin to show effects of packing inhomogeneities. At the higher flow-rate, two sets of peaks with a substantial amount of tailing are obtained, likely as a result of the formation of channels in the packing. At this high flow-rate and low precompression pressure, a significant portion of the cartridge must be expanded and a poor performance is observed. After completing a series of runs operating at this low precompression level, the original precompression pressure of 225 psig was restored. The resulting profiles are shown in Fig. 10. Remarkably, most of the damage generated by operating at 100 psig appears to have been repaired and now relatively sharp peaks are obtained for each component. However, substantially higher HETPs and increased

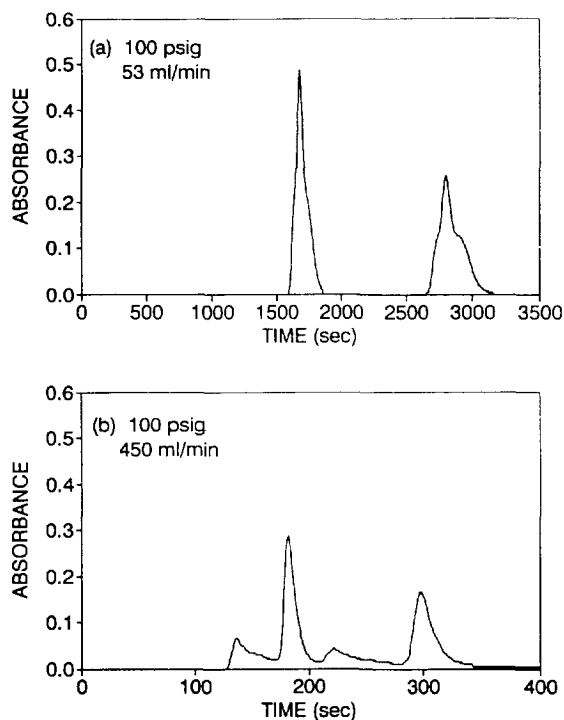


Fig. 9. Elution profiles for methyl and ethyl paraben with the Hyperprep cartridge lowering the precompression setting to 100 psig. (a)  $H = 0.015$  cm and  $\alpha_s = 2.4$  for methyl paraben,  $H = 0.016$  cm and  $\alpha_s = 2.0$  for ethyl paraben, (b)  $H$  and  $\alpha_s$  values not determined.

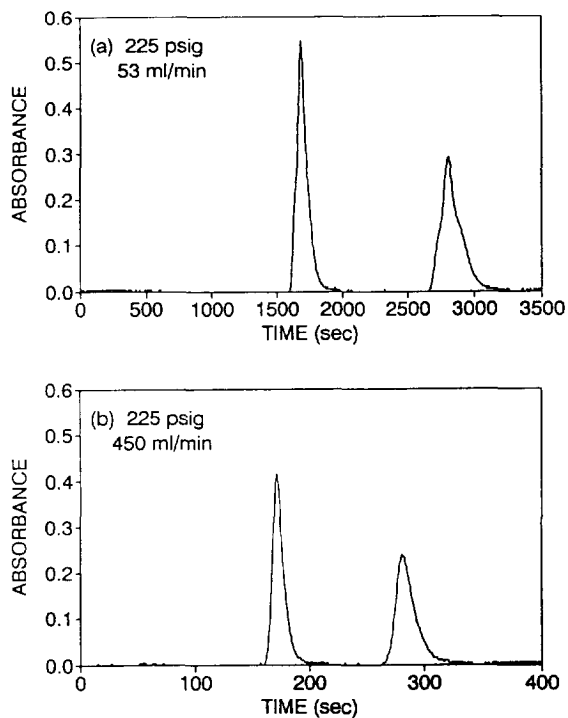


Fig. 10. Elution profiles for methyl and ethyl paraben with the Hyperprep cartridge after reapplying the precompression setting of 225 psig. (a)  $H = 0.012$  cm and  $\alpha_s = 1.2$  for methyl paraben,  $H = 0.013$  cm and  $\alpha_s = 1.7$  for ethyl paraben, (b)  $H = 0.015$  cm and  $\alpha_s = 1.8$  for methyl paraben,  $H = 0.017$  cm and  $\alpha_s = 1.9$  for ethyl paraben.

asymmetry factors are obtained relative to the initial runs shown in Fig. 8. Precompression settings up to 400 psig were used in an attempt to totally restore the initial efficiency. However, for none of these settings was a better elution profile obtained than those depicted in Fig. 8. Some irreversible damage apparently was done when the column efficiency was destroyed by operating at too low a precompression level.

#### 4. Conclusions

Preparative-scale radial compression chromatography columns have been found to possess efficiencies close to those of analytical-scale columns when operated with an adequate level of precompression. The relationship between radial compression pressure and internal column

pressure is such that, under flow conditions, the net compressive force is larger near than column exit than near the entrance. When the system is operated with a fixed amount of compression, as the mobile phase flow-rate is increased the minimum net compressive force on the packing is reduced. If the precompression level is low, a portion of the packed cartridge can actually become expanded, relative to its uncompressed size. A precompression level that in operation will keep the cartridge fully compressed can be safely selected as equal to one half the column backpressure that is generated for a given operating flow-rate. Lower precompression levels can lead to an outward expansion of the cartridge at high flow-rates. We studied two different chromatographic media. The first, comprising irregular  $C_{18}$  silica, was quite insensitive

to the precompression level. It yielded efficiencies equal to those of an analytical-scale column, stably over long periods of time. The second media, comprising spherical monodispersed  $C_{18}$  silica of a smaller size than the first media, yielded efficiencies close to those of an analytical-scale column only when operated at the manufacturers recommended precompression level. As shown for example by Yun and Guiochon [13], flow non-uniformities across the radius of HPLC columns can have dramatic effects on the efficiency. The close agreement between our preparative-scale and analytical-scale results, however, suggests that although packing non-uniformities may exist in the axial direction of radial compression columns, these columns are homogeneous in the radial direction. At low precompression levels, severe channeling apparently occurred, leading to a nearly complete destruction of a model separation. Remarkably, however, application of increasing levels of radial compression lead to a healing, albeit not complete, of the damage done by operating the column at low precompression levels, enabling an almost complete recovery of the original chromatographic efficiency.

Consistent with previous studies by Carta and Stringfield and Sarker and Guiochon [8,9], it appears that the radial compression technology provides hardware adequate for a predictable scale-up of HPLC. Operation of these systems is only slightly more complicated than those of conventional columns and has the advantage that reliable cartridges packed by the manufacturer can easily and rapidly be replaced in the unit. A simple criterion developed in this paper allows one to set a safe level of column precompression that will yield a stable and efficient operation.

### Acknowledgements

This research was supported in part by Biotage, Inc., and by the Virginia Center for Innovative Technology. We are grateful to Biotage for the loan of the KP100 unit and of columns used in this study and to Kevin Holland for insightful discussions.

### List of symbols

$d_p$  particle diameter

$D$	mobile phase solute diffusivity
$E$	cartridge modulus of elasticity
$E'$	modulus of elasticity of cartridge shell
$h$	reduced HETP
$H$	height equivalent to a theoretical plate (HETP)
$L$	column length
$N$	plate count
$P_b$	pressure of radial compression fluid
$P_b^0$	precompression pressure
$P_c$	column backpressure
$P_i$	internal column pressure
$R$	cartridge radius
$\Delta R$	change in cartridge radius
$u$	superficial velocity
$v$	linear interstitial velocity
$z$	axial coordinate
$z'$	position in column where $P_i = P_b$
$\alpha_s$	peak asymmetry factor
$\epsilon$	apparent column void fraction
$\mu$	mobile phase viscosity

### References

- [1] M. Verzele, M. De Coninck, J. Vindevogel and C. Dewaele, *J. Chromatogr.*, 450 (1988) 47.
- [2] H. Colin, P. Hilarieau and J. de Tournemire, *LG·GC*, 8 (1990) 302.
- [3] G.B. Cox, *LG·GC*, 8 (1990) 690.
- [4] M. Verzele, *Anal. Chem.*, 62 (1990) 265A.
- [5] M. Sarker and G. Guiochon, *LC·GC*, 12 (1994) 302.
- [6] S. Marme, M. Hallmann, K.K. Unger, E. Baumeister, K. Albert and E. Bayer, in M. Perrut (Editor), *Proceedings of the 9th International Symposium on Preparative and Industrial Chromatography*, Societe Francais de Chimie, Paris, France, 1992, p. 135.
- [7] D. Train, *Trans. Instn. Chem. Engrs.*, 35 (1957) 258.
- [8] G. Carta and W.B. Stringfield, *J. Chromatogr. A*, 658 (1994) 407.
- [9] M. Sarker and G. Guiochon, *J. Chromatogr. A*, 683 (1994) 293.
- [10] R.B. Bird, W.E. Stewart and E.N. Lightfoot, *Transport Phenomena*, Wiley, New York, NY, 1960, p. 196.
- [11] D.P. Gervais, Masters Thesis, University of Virginia, Charlottesville, VA, 1994.
- [12] V. Huss, J.L. Chevalier and A.M. Siouffi, *J. Chromatogr.*, 500 (1990) 241.
- [13] T. Yun and G. Guiochon, *J. Chromatogr. A*, 672 (1994) 1.